

Analytic treatment of CRIB Quantum Memories for Light using Two-level Atoms

J. J. Longdell

*Department of Physics, University of Otago, Dunedin, New Zealand**

G. Hétet and P. K. Lam

ARC COE for Quantum-Atom Optics, Australian National University, Canberra, ACT 0200, Australia

M. J. Sellars

Laser Physics Centre, RSPHysSE, Australian National University, Canberra, ACT 0200, Australia

(Dated: 1 July 2008)

It has recently been discovered that the optical analogue of a gradient echo in an optically thick material could form the basis of an optical memory that is both completely efficient and noise free. Here we present analytical calculation showing this is the case. There is close analogy between the operation of the memory and an optical system with two beam splitters. We can use this analogy to calculate efficiencies as a function of optical depth for a number of quantum memory schemes based on controlled inhomogeneous broadening. In particular we show that multiple switching leads to a net 100% retrieval efficiency for the optical gradient echo even in the optically thin case.

I. INTRODUCTION

The ability to store and recall quantum states of light as coherences in atomic media is currently being actively pursued. Such quantum memories would find use both in optical based quantum computation [1] and long distance quantum communication [2].

Many of the current quantum memory approaches involve the use of three level atomic systems, and store quantum information between two quasi ground states [3, 4, 5, 6, 7]. Quantum states have been stored and recalled using this approach [3, 8, 9, 10]. Three level schemes are particularly well suited to gaseous atomic systems where significant optical depths can be obtained for the optical transitions due the allowed transitions and long coherence times can be obtained for the ground state coherences. Rare earth ion doped solids at cryogenic temperatures have much higher atom densities and allow reasonable optical thickness to be obtained from ensembles of weak oscillators. These weak oscillators can have correspondingly long coherence times. This means that approaches involving only two level atoms can be considered. Sangouard et al. [11] showed that in principle 54% efficiency can be achieved from a controlled reversible inhomogeneous broadening (CRIB) echo [6, 7] with two level atoms, in the case where the broadening mechanism is ‘transverse’, that is not correlated with position along the optical path. The efficiency was limited by reabsorption, as the sample is made more optically thick, which is required to absorb the input pulse, more of the echo gets absorbed before it can make it out of the sample. Shortly afterward it was shown that the optical gradient echo or “longitudinal” CRIB echo [12], the only CRIB echo that has so far been reported experimentally, did not suffer from reabsorption problems and offered noise free, potentially 100% efficient storage [13]. An attractive property of these echo based techniques is that time bandwidth product scales better with optical depth [2, 14]. Indeed storing and recalling multiple pulses has been demonstrated for CRIB echo memories [15] but this has proved difficult for EIT.

Following on from [13] here we present analytic theory of the optical gradient echo or “longitudinal CRIB” echo. Analytic solutions of the Maxwell-Bloch equations are derived for a pulse of light interacting with ensemble of atoms, where the resonant frequency atoms varies linearly with the propagation distance. After the input pulse atomic coherence dephases due to the different resonant frequencies of the atomic ensemble. If the detunings of each of the atoms are reversed the ensemble rephases and produces an echo. In the case where the medium is optically thick the echo is totally efficient. Indeed, we show very close analogy between a gradient echo memory and a pair of beamsplitters. We use this analogy to calculate the efficiency of the longitudinal echo for optically thin samples. Multiple switching and a number of memories operated in series can also be easily treated using this beamsplitter analogy. As transverse broadening can be considered as the limit of many stacked optically thick transverse broadening. Transverse broadening can be treated using the same approach. We reproduce previous results for the efficiency of transverse CRIB echoes [11] and extend to the case of multiple switching.

*Electronic address: jevon.longdell@otago.ac.nz

II. THEORY

We consider the interaction of a collection of two-level atoms with a light field where a detuning of the atoms that is linearly dependent on their position can be introduced. We shall assume that the area of the incoming pulses is much less than that of a π pulse. This enables us to treat the atoms as harmonic oscillators. Before the detuning of the ions are flipped, the Maxwell-Bloch equations in the frame at the speed of light are [16]

$$\frac{\partial}{\partial t}\alpha(z, t) = -(\gamma + i\eta z)\alpha(z, t) + igE(z, t) \quad (1)$$

$$\frac{\partial}{\partial z}E(z, t) = iN\alpha(z, t) \quad (2)$$

Where E represents the slowly varying envelope of the optical field; α the polarization of the atoms; N the atomic density; g the atomic transition coupling strength; γ the decay rate from the excited state and ηz the detuning from resonance. We shall assume that the process happens fast compared to the atomic decay rate and will take $\gamma = 0$.

After the detuning of the ions is flipped to recall the light pulse the Maxwell-Bloch equations describing the dynamics are the same as above except the sign of the $i\eta z$ term in 1 is flipped leading to (with $\gamma = 0$)

$$\frac{\partial}{\partial t}\alpha(z, t) = -i\eta z\alpha(z, t) + igE(z, t) \quad (3)$$

$$\frac{\partial}{\partial z}E(z, t) = iN\alpha(z, t) \quad (4)$$

As mentioned above, although the treatment here is classical, the linearity of Eqs. (1,2,3,4) ensures that exactly the same analysis would be true for operator valued α and E . The only added noise in the output pulses will be the vacuum noise added to preserve commutation relations in much the way as light interacting with a beam-splitter. Our results will thus hold for quantum mechanical fields also.

The domain over which these equations will be solved is illustrated in Fig. 1. The boundary conditions are the input pulse $E(z = -z_0, t) = f_{\text{in}}(t)$ and the initial state of the atoms. We shall assume that the atoms start in their ground state so that $\alpha(z, t = -\infty) = 0$. By propagating forward in both z and t from these boundary conditions one could determine the final state of the atoms and the light exciting the sample at $z = z_0$. Ideally the procedure would result in an output pulse, $E(z = +z_0, t) = f_{\text{out}}(t)$ that has the same energy and is closely related to the input pulse, and that at the end of the process all the atoms are left in their ground states, $\alpha(z, t = +\infty) = 0$. It should be noted that we are dealing with the situation where there is no decay of the atomic states, so in order for $\alpha(z, t = +\infty) = 0$ the atoms must be left in their ground states at the end of the retrieval process, it cannot happen via decay of the atomic states.

Rather than propagating forward all the way from our boundary conditions at $z = -z_0$ and $t = -\infty$ to arrive at expressions for $z = z_0$ and $t = +\infty$ we will take a different approach that better makes use of the symmetry of the situation. We first solve for the behavior in Region A using the boundary conditions $\alpha(z, t = -\infty) = 0$ and $E(z = -z_0, t < 0) = f_{\text{in}-}(t)$. This analysis will give us expressions for E and α at the time when the detunings are flipped ($\alpha(z, t = 0)$ and $E(z, t = 0)$) as well an expression for the light that leaves the sample before the field is flipped ($E(z = +z_0, t < 0) = f_{\text{out}-}(t)$).

We then carry out what turns out to be a very similar analysis. Working in Region B, we start with an arbitrary form output pulse ($E(z = +z_0, t > 0) = f_{\text{out}+}(t)$) and the requirement that the atoms end up in their ground states ($\alpha(z, t = \infty) = 0$) and then we work out what is needed from the other two boundary conditions ($E(z = -z_0, t > 0)$ and ($\alpha(z, t = 0)$ and $E(z, t = 0)$) in order for these outcomes to occur. By comparing these required boundary conditions with those that actually occur we show that in the case of an optically thick sample the storage is completely efficient. For the case of an optically thin sample we can calculate how efficient the process will be.

The analysis of the behavior in Region A is as follows: First Eq. 1 is integrated to give

$$\begin{aligned} \alpha_a(z, t) &= ig \int_{-\infty}^t dt' e^{-i\eta z(t-t')} E_a(z, t') \\ &= ig \int_{-\infty}^{\infty} dt' H(t-t') e^{-i\eta z(t-t')} E_a(z, t') \end{aligned} \quad (5)$$

here H denotes the Heaviside step function. The above expression is in the form of a convolution, taking the Fourier transform gives a product.

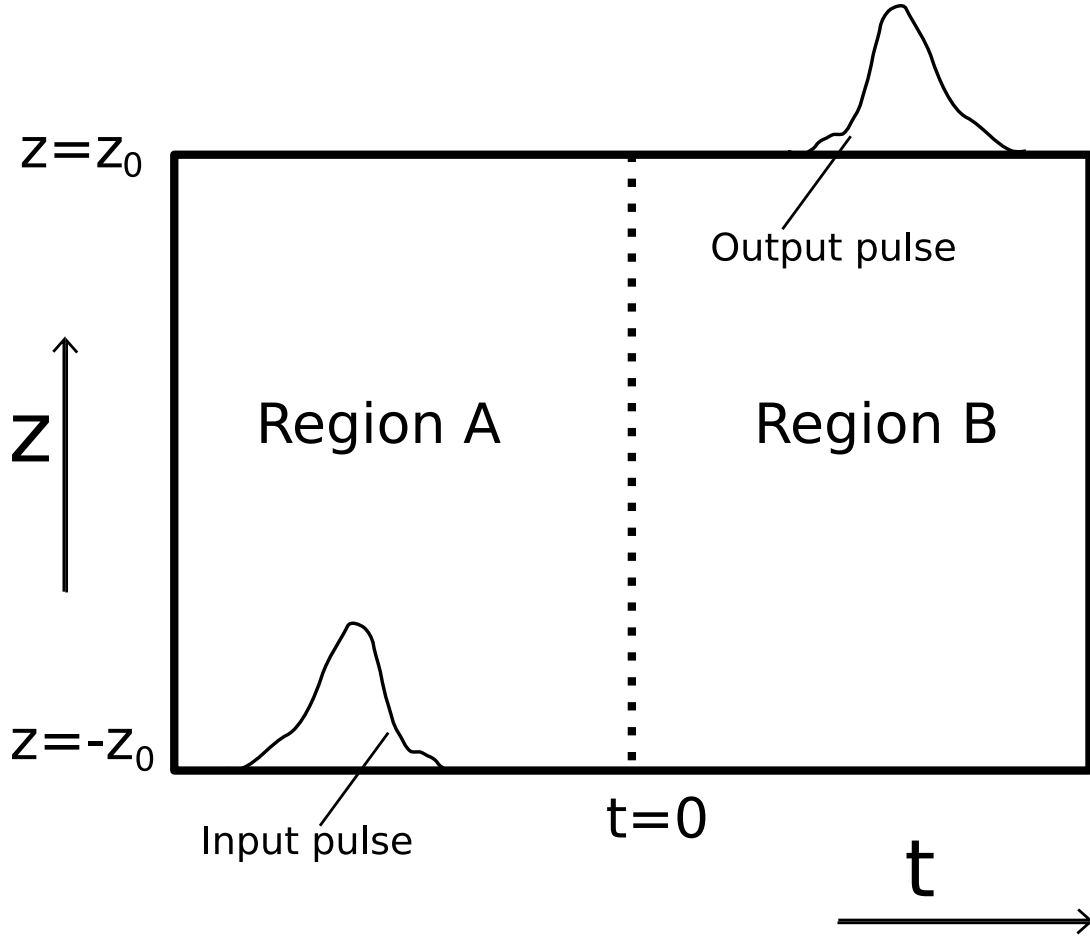


Figure 1: The domain over which the Maxwell-Bloch equations are solved. Each horizontal slice represents one position in the sample of atoms as a function of time. The light enters the sample at $z = -z_0$ and leaves at $z = +z_0$. The dotted line represents the point in time at which the detunings of the ions are flipped. In Region A the dynamics are described by Eqns. 1 and 2, in Region B the dynamics are described by Eqns. 3 and 4.

$$\alpha_a(z, \omega) = igE_a(z, \omega) \left(\frac{1}{i(\omega + \eta z)} + \pi\delta(\omega + \eta z) \right) \quad (6)$$

Substituting this in Eq. 2 we get

$$\partial_z E_a(z, \omega) = -g^2 N \left(\frac{1}{i(\omega + \eta z)} + \pi\delta(\omega + \eta z) \right) E_a(z, \omega) \quad (7)$$

Integrating this equation we have

$$\begin{aligned} E_a(z, \omega) &= E_a(z = -z_0, \omega) \exp \int_{-z_0}^z dz' - g^2 N \left(\frac{1}{i(\omega + \eta z')} + \pi\delta(\omega + \eta z') \right) \\ &= F_{\text{in-}}(\omega) \exp(-\beta\pi(H(\omega + \eta z) - H(\omega + \eta z_0))) \left| \frac{\omega + \eta z}{\omega + \eta z_0} \right|^{i\beta} \end{aligned} \quad (8)$$

where $\beta = \frac{g^2 N}{\eta}$.

It can be seen that the amplitude of each spectral component is attenuated by a factor $\exp(-\pi\beta)$ after traveling past the position in the sample where it is resonant with the atoms. It also receives a phase shift as it travels through the sample.

We make the assumption that the spectral coverage of the sample is large compared to the optical depth. That is for each frequency of interest ω in our input signal we have $\beta\omega \ll \eta z_0$ in which case our expression for $E_a(z, \omega)$ takes the form

$$E_a(z, \omega) = F_{\text{in}-}(\omega) \exp(-\beta\pi H(\omega + \eta z)) \left| \frac{\omega + \eta z}{\eta z_0} \right|^{i\beta} \quad (9)$$

Substituting $z = +z_0$ in the above equation one finds that the transmitted pulse is equal to the the incident pulse multiplied by an attenuation factor $\exp(-\beta\pi)$.

$$f_{\text{out}-}(t) = f_{\text{in}-}(t)e^{-\beta\pi} \quad (10)$$

In the limit of large β no light is transmitted and all remains in the material during the period $t < 0$.

Integrating Eq. 9 with respect to ω gives an expression for $E_a(z, t = 0)$ in the form of a convolution Fourier transforming along the spatial coordinate we get.

$$E_a(k, t = 0) = -f_{\text{in}-}\left(-\frac{k}{\eta}\right) \text{sgn}(k)\beta \left| \frac{k}{\eta} \right|^{-1+i\beta} \Gamma(i\beta) \left(\left| \frac{k}{\eta} \right| \cosh\left(\frac{\pi\beta}{2}\right) + \frac{k}{\eta} \sinh\left(\frac{\pi\beta}{2}\right) \right) \quad (11)$$

Here $f_{\text{in}}(k/\eta)$ is the input field at the time $\tau = k/\eta$ and $\Gamma(\xi)$ is the gamma function. An expression for α at the time the field was flipped can easily be obtained from the above result along with Eq. 2.

We now turn our attention to Region B and calculate α_b and E_b in that region subject to our desired boundary conditions $\alpha_b(z, t = \infty) = 0$, $E_b(z = z_0, t) = f_{\text{out}+}(t)$. The output field $f_{\text{out}+}(t)$ is at this stage undetermined.

Solving Eq. 3 subject to the output condition $\alpha_b(z, t = \infty) = 0$ gives

$$\begin{aligned} \alpha_b(z, t) &= ig \int_{+\infty}^t dt' e^{i\eta z(t-t')} E_b(z, t') \\ &= -ig \int_{-\infty}^{\infty} dt' H(t' - t) e^{-i\eta z(t'-t)} E_b(z, t') \end{aligned} \quad (12)$$

Fourier transforming gives

$$\alpha_b(z, \omega) = -ig E_b(z, \omega) \left(\frac{i}{(\omega - \eta z)} + \pi\delta(\omega - \eta z) \right) \quad (13)$$

Substituting this in Eq. 4 and integrating gives

$$\begin{aligned} E_b(z, \omega) &= E_b(z = z_0, \omega) \exp \int_{+z_0}^z dz' g^2 N \left(\frac{i}{(\omega - \eta z')} + \pi\delta(\omega - \eta z') \right) \\ &= F_{\text{out}+}(\omega) \exp(-\beta\pi(H(\omega - \eta z) - H(\omega - \eta z_0))) \left| \frac{\omega - \eta z}{\omega - \eta z_0} \right|^{i\beta} \end{aligned} \quad (14)$$

In a similar manner to in Region A, in the limit of large z_0 this can be approximated.

$$E_b(z, \omega) = F_{\text{out}+}(\omega) \exp(-\beta\pi H(\omega - \eta z)) \left| \frac{\omega - \eta z}{\eta z_0} \right|^{i\beta} \quad (15)$$

From the above expression $E_b(z = -z_0, t)$ can be calculated resulting in

$$f_{\text{in}+}(t) = f_{\text{out}+}(t)e^{-\beta\pi} \quad (16)$$

Also from Eq. 15 one can find an expression for $E_b(k, t = 0)$:

$$E_b(k, t = 0) = f_{\text{out}+}\left(-\frac{k}{\eta}\right) \text{sgn}(k)\beta \left| \frac{k}{\eta} \right|^{-1-i\beta} \Gamma(-i\beta) \left(\left| \frac{k}{\eta} \right| \cosh\left(\frac{\pi\beta}{2}\right) + \frac{k}{\eta} \sinh\left(\frac{\pi\beta}{2}\right) \right) \quad (17)$$

Equations 16 and 17 give conditions, that if satisfied, will lead to a particular output pulse $f_{\text{out}+}(t)$ and all the atoms being left in the ground state at the end of the process. From Eq. 16 and comparing Eqns. 11 and 17 we see that if an auxiliary input pulse is applied an output pulse related to our input pulse by

$$f_{\text{out}+}^+(t) = -f_{\text{in}}^-(t)|t|^{2i\beta} \frac{\Gamma(i\beta)}{\Gamma(-i\beta)}. \quad (18)$$

Because $|t|^{2i\beta}\Gamma(i\beta)/\Gamma(-i\beta)$ has a modulus of 1 for all t , it can be seen that the envelope of the output pulse is a time reversed version of the input. The required auxiliary pulse is given by 17, the practical usefulness of the memory would of course be greatly hampered by the need for this auxiliary input pulse. Which must be an attenuated copy of the output pulse applied at the same time as the output pulse. However in the situation where the sample is optically thick, $\exp(-\beta\pi) \ll 1$, the required input pulse is zero. When arriving at Eq. 18 one only needs to ensure that for $t = 0$ the values for E match, the values for α will then also match because of Eqns. 2 and 4.

The phase between the input pulse and the output pulse changes across the pulse an amount given by $2\beta \log(t_{\text{end}}/t_{\text{start}})$ where t_{start} and t_{end} are the start and end times times for the output pulse. This will be a modest phase shift in most situations where the memory might be used. A value for β of 2 would provide sufficient optical depth for 99.999% efficiency, with this and 2 for $t_{\text{end}}/t_{\text{start}}$ the phase shift across the pulse would be less than π . This phase shift could be corrected for by some time dependent change in the optical path length, for instance a mirror mounted on a piezo or and electro optic modulator. Alternately two memories could be used in series with the initial frequency gradients opposite for each memory, the phase shifts of the two memories would then cancel.

III. EFFICIENCY AND ANALOGUE BEAMSPLITTERS

The fact that we can still get the desired output pulse with an optically thin sample by applying an auxiliary input pulse may not be all that helpful in the practical operation of the memory. It does however, along with the linearity of the differential equations, enable one to determine the effect of the memory in the optically thin regime. The difference between the true output pulse when working in the optically thin regime and the ideal case is equal to the effect of applying the auxiliary pulse alone. There is a close analogy between the operation of the memory in the finite optical depth regime and a beam splitter. An optical beam splitter takes a pairs of optical modes and outputs linear combinations of these modes. The action of the memory for both the times $t < 0$ and $t > 0$ can be reduced to that of a beam splitter, these are illustrated in Fig. 2 . Each of the two beamsplitters have two input and two output ports. For the left hand beamsplitter bottom input port, labeled $f_{\text{in}}^-(t)$ and the mode of interest is the temporal mode of the optical wavepacket that we wish to store. The top, output port of the left hand beam splitter, labeled $f_{\text{out}}^-(t)$ for this represents the light that is transmitted through the sample, from Eq. 10, we can see that this transmitted light has the same temporal mode as the input light and that the amplitude transmittivity of our analogue beam splitter will be $\exp(-\beta\pi)$. The left hand input port and the right hand output ports of the two beamsplitters aren't optical modes but instead the beamsplitter acts on, and produces, 'polariton' excitations that have both an atomic and optical component. Like the polaritons considered in electromagnetically induced transparency (EIT) [17] these are combinations of photon and atom excitations. Unlike EIT polaritons optical gradient polaritons propagate in reciprocal space, to higher spatial frequencies, rather than propagating along the propagation direction [14].

The left hand port of the left hand beamsplitter represents the initial state of the optical field in the sample and the atoms before the input pulse is applied in for the case of our memory, during the operation of the memory this state will be a vacuum state. The right hand output mode of the first beamsplitter represents the mode of the excitation in the sample at the time the field is switched ($t = 0$). The optical component of mode function is given by Eq. 11 and the atomic part can be found from Eq. 2. One explanation for why the memory works is that output polariton mode for the left hand beamsplitter that represents the ($t < 0$) evolution matches the input polariton mode for righthand beamsplitter that represents the ($t > 0$) evolution. So long as we choose input and output optical modes for the given by equations Eq. 16 and 18. The amplitude transmittivity of this second beamsplitter is given by $\exp(-\beta\pi)$.

In order to have an efficient memory we would require excitation fed into the $f_{\text{in}}^-(t)$ port of the network shown in Fig. 2 to be directed entirely to the $f_{\text{out}}^+(t)$ port . This requires high reflectivity for our analogue beamsplitters or equivalently large optical depth. The beamsplitter analogy easily enables calculation of the efficiency of the echo process as a function of optical depth. Because both beamsplitters have an amplitude transmittivity of $\exp(-\beta\pi)$ we end up efficiency for the echo given by

$$\text{Efficiency} = (1 - \exp(-2\beta\pi))^2$$

This result agrees with the numerical simulations we have presented previously [13]. From the beamsplitter analogue one can also see immediately where the rest of the incident energy goes, $\exp(-2\beta\pi)$ was transmitted by the sample and $\exp(-2\beta\pi)(1 - \exp(-2\beta\pi))$ remains in the sample.

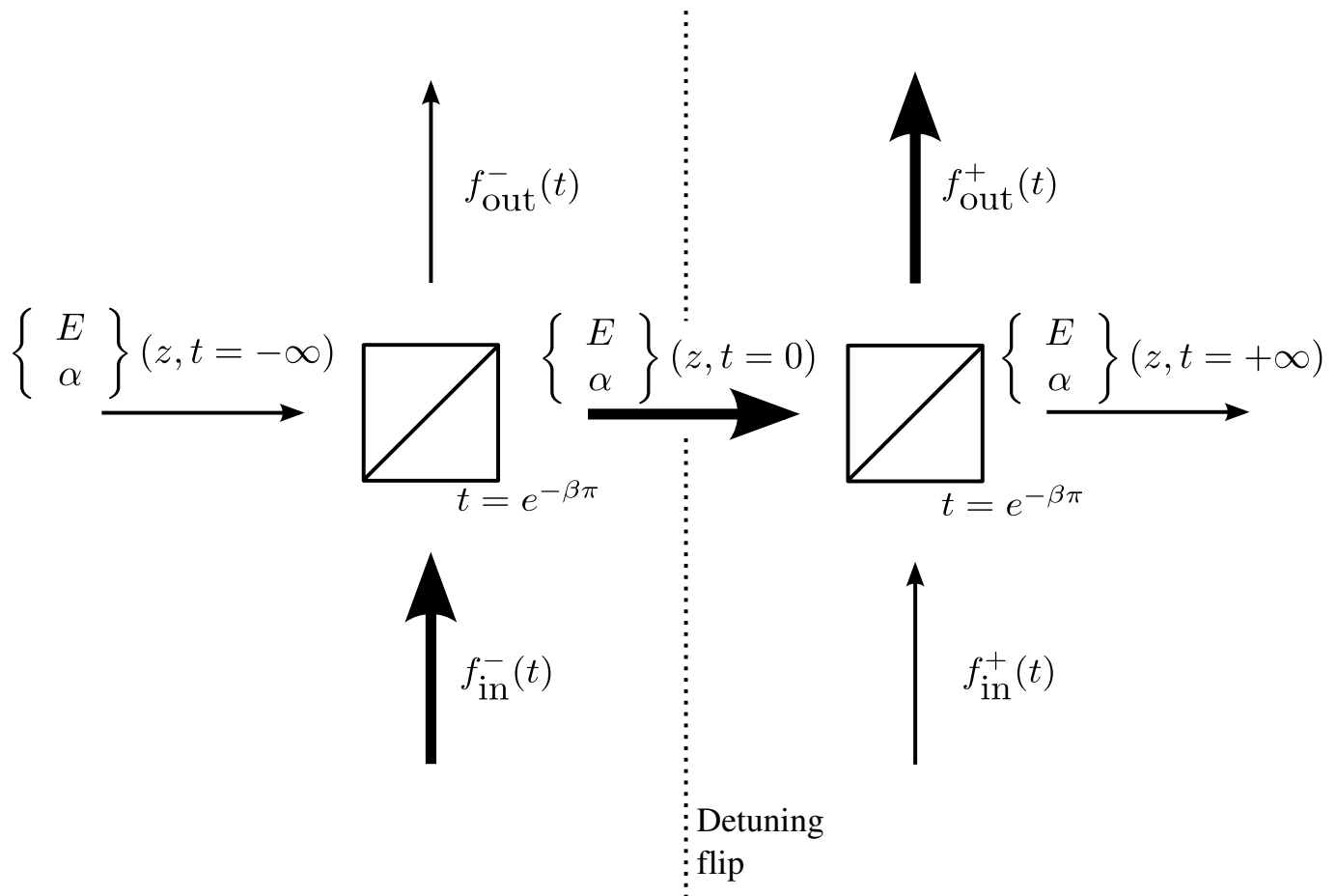


Figure 2: The optical gradient echo memory represented as a pair of beam splitters. The bold arrows represent the flow of energy in the optically thick case. The spatial and temporal modes that correspond to the each port of the beam splitter is discussed in the text.

IV. TRANSVERSE BROADENING AND MULTIPLE SWITCHING.

Initial theoretical treatments of the efficiency of two-level controlled reversible inhomogeneous broadening (CRIB) echoes [11] investigated situations where the controlled detunings of the ions were not correlated with the position the atom. Such transverse broadening would arise from a microscopic broadening mechanism. This situation can be modeled by a large number of optically thin gradient echo sub-memories in series. The relevant network of analogue beamsplitters is shown in Fig. 3. If there are M sub memories, the transmitted input pulse will be attenuated by $\exp(-2\beta\pi M)$. There are M paths a photon can take from the input pulse $f_{in}^{-}(t)$ to the output pulse $f_{out}^{+}(t)$, each of which involves two reflections and $M - 1$ transmissions from our analogue beamsplitters. Because the echo from each sub-memory combines in phase with that from the previous memory these paths all combine constructively to give an efficiency for the echo of $M^2(1 - \exp(-2\beta\pi))^2 \exp(-2\beta\pi(M - 1))$. Taking the limit where each sub-memory is optically thin (β small) we arrive at an efficiency for the memory with microscopic broadening

$$\text{Efficiency} = 4\beta^2\pi^2 M^2 \exp(-2\beta\pi M) = d^2 e^{-d}$$

Here $d = 2\beta\pi M$ is the optical depth, (the logarithm of the ratio of the energies of the incident and transmitted pulses). This result is the same as that derived in [11] by solution of the Maxwell-Bloch equations.

Another situation to which our beamsplitter analogy can be applied is multiple switching of the broadening, both for longitudinal and transverse broadenings. If the broadening is switched in polarity after the first echo the excitation remaining in the sample will again be rephased leading to another echo. Multiple echoes of the original input pulse can be created in this way. The analogue beamsplitter network for multiple switching in a gradient echo is shown in Fig. 4, from this network one can see that the fraction of the input energy coming out in the k^{th} echo is

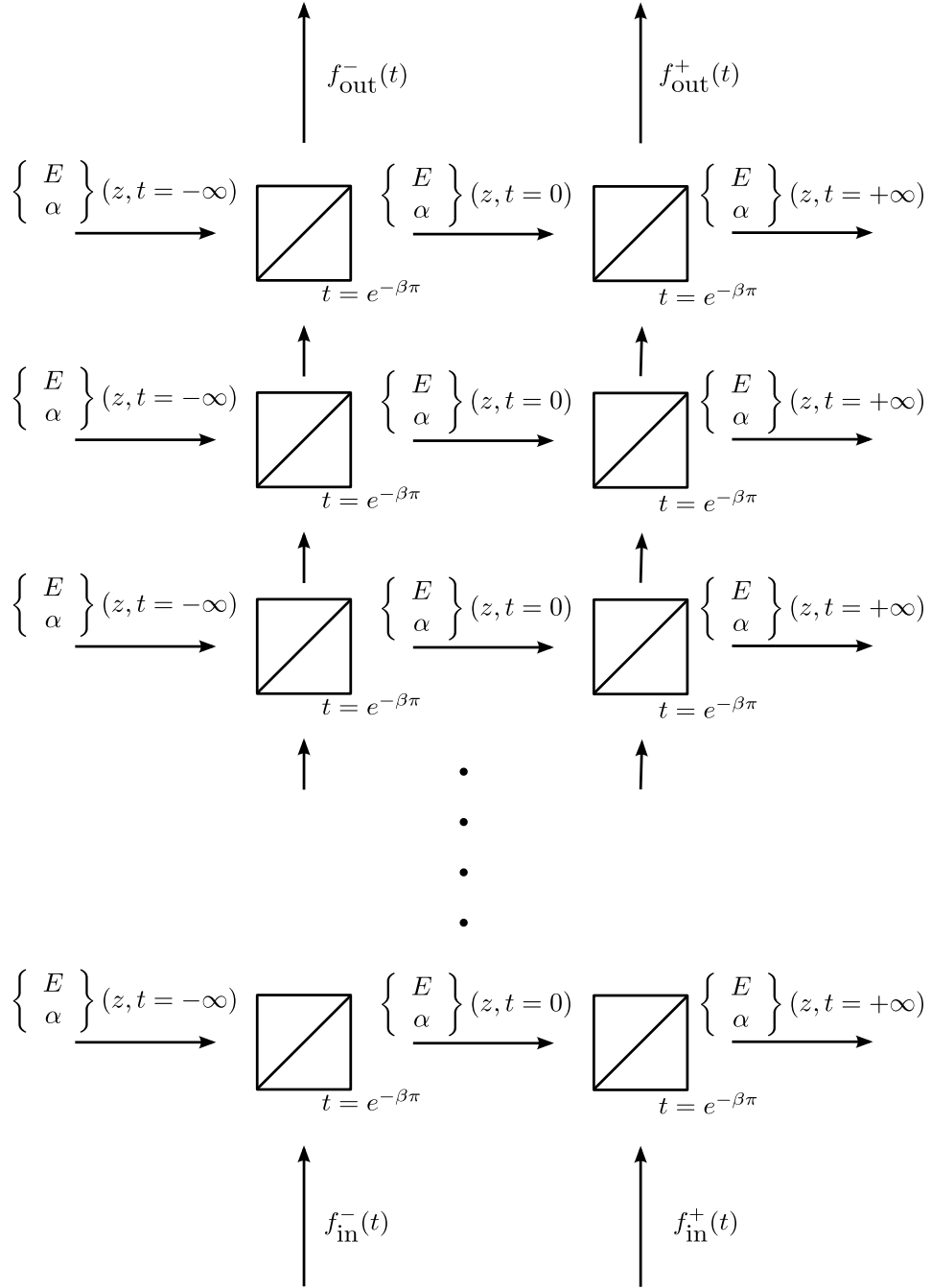


Figure 3: Network of analogue beamsplitters relevant to a transverse CRIB memory modeled as a large number of optically gradient echo memories.

$(1 - \exp(-2\beta\pi))^2 \exp(-2\beta\pi(k-1))$. From the beamsplitter network it can be seen that with multiple switching the energy eventually leaves the sample in either as the transmitted pulse or as one of the echoes. The efficiencies of the echos as a function of β are plotted in Fig. 5.

The beam splitter analogy can be extended further to the case of multiple switching from a system with microscopic broadening. The network of analogue beam splitters in this situation is similar to Figs. 3 but with a 2D array of beam splitters. The amplitude of each of the multiple echos can be calculated by summing the amplitudes of all the possible paths through the beamsplitter network. This leads to the following expression for the portion of the incident energy that is output as the p^{th} echo

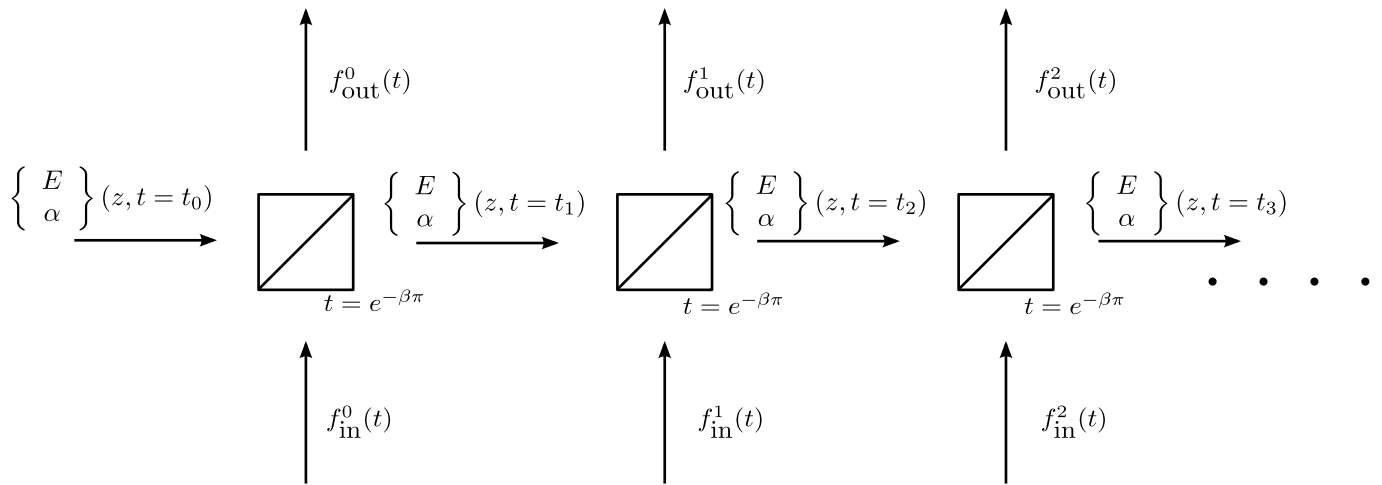


Figure 4: Network of analogue beamsplitters relevant to an optical gradient echo memory where the field is switched a number of times

$$e_p = t^{M+p} \left| \sum_{k=1}^p \binom{p-1}{k-1} \frac{1}{k!} \left(-\frac{r^2}{t^2} \right)^k \right|^2$$

Here $r = (1 - \exp(-2\beta\pi))$ and $t = \exp(-\beta\pi)$ are the amplitude transmission and reflection coefficients of the analogue beamsplitters. Taking the limit a large number of optically thin memories. We get the following expression for the efficiency of the p^{th} echo as

$$e_p = \exp(-d) \left| \sum_{k=1}^p \binom{p-1}{k-1} \frac{1}{k!} (-d)^k \right|^2$$

where d is the optical depth. As is shown in Fig. 6 combined efficiencies significantly greater than 54% can be achieved with multiple switching.

V. CONCLUSION

In conclusion we have presented an analytic treatment of the optical gradient echo, or longitudinal CRIB echo. We have shown that it is completely efficient in the case of large optical depth and that recall efficiencies of 100% can also be obtained for optically thin samples by multiple switching. By modeling a system with transverse CRIB by a large number of optically thin gradients can calculate echo efficiencies in this case also. As has been shown elsewhere the maximum echo efficiency is $4/e^2 \approx 54\%$. Multiple switching can improve this overall efficiency with efficiencies of $> 90\%$ possible for the sum of the first 100 echoes.

-
- [1] E. Knill, R. Laflamme, and G. J. Milburn, *Nature* **409**, 46 (2001).
 - [2] C. Simon, H. de Riedmatten, M. Afzelius, N. Sangouard, H. Zbinden, and N. Gisin, *Phys. Rev. Lett.* **98**, 190503 (2007).
 - [3] B. Julsgaard, J. Sherson, J. I. Cirac, J. Fiurasek, and E. S. Polzik, *Nature* **432**, 482 (2004).
 - [4] M. Fleischhauer and M. D. Lukin, *Phys. Rev. A* **65**, 022314 (2002).
 - [5] A. V. Gorshkov, A. André, M. D. Lukin, and A. S. Sørensen, *Phys. Rev. A* **76**, 033806 (2007).
 - [6] S. A. Moiseev and S. Kroll, *Phys. Rev. Lett.* **87**, 173601 (2001).
 - [7] B. Kraus, W. Tittel, N. Gisin, M. Nilsson, S. Kroll, and J. I. Cirac, *Phys. Rev. A* **73**, 020302(R) (2006).
 - [8] T. Chanelire, D. N. Matsukevich, S. D. Jenkins, S.-Y. Lan, T. A. B. Kennedy, and A. Kuzmich, *Nature* **428**, 833 (2005).
 - [9] M. D. Eisaman, A. Andr, F. Massou, M. Fleischhauer, A. S. Zibrov, and M. D. Lukin, *Nature* **438**, 837 (2005).
 - [10] J. Appel, E. Figueroa, D. Korystov, M. Lobino, and A. I. Lvovsky, *Phys. Rev. Lett.* **100**, 093602 (2008).

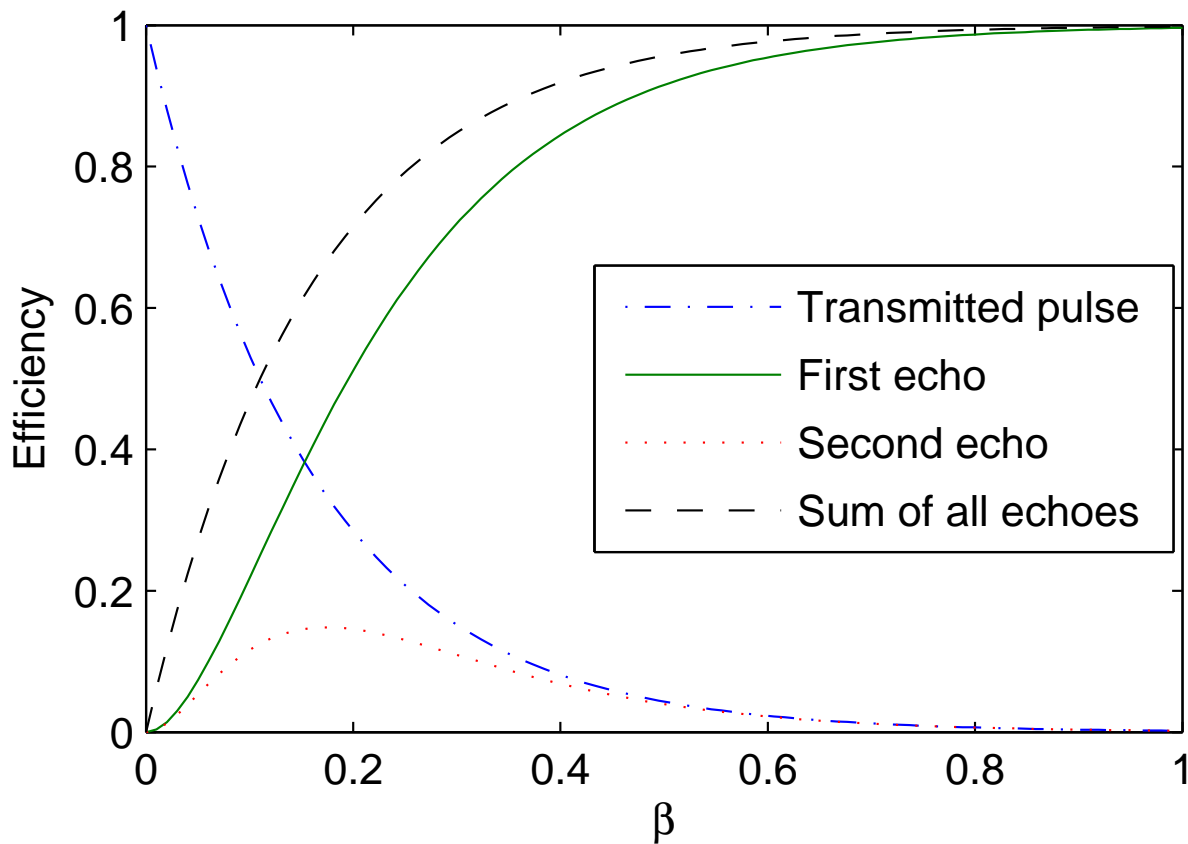


Figure 5: (Color online) Echo efficiency for an optical gradient echo as a function of β showing the effect of multiple switching. The ratio of the energies of the input and transmitted pulse is given by $\exp(-2\pi\beta)$.

- [11] N. Sangouard, C. Simon, M. Afzelius, and N. Gisin, *Phys. Rev. A* **75**, 032327 (2007).
- [12] A. L. Alexander, J. J. Longdell, M. J. Sellars, and N. B. Manson, *Phys. Rev. Lett.* **96**, 043602 (2006).
- [13] G. Hetet, J. J. Longdell, A. L. Alexander, P. K. Lam, and M. J. Sellars, *Phys. Rev. Lett.* **100**, 023601 (2008).
- [14] G. Hétet, J. J. Longdell, M. J. Sellars, P. K. Lam, and B. C. Buchler, *Bandwidth and dynamics of the gradient echo memory* (2008), arXiv:0801.3860.
- [15] A. L. Alexander, J. J. Longdell, M. J. Sellars, and N. B. Manson, *J. Lumin* **127**, 94 (2007).
- [16] M. D. Crisp, *Phys. Rev. A* **1**, 1604 (1970).
- [17] M. Fleischhauer and M. D. Lukin, *Phys. Rev. Lett.* **84**, 5094 (2000).

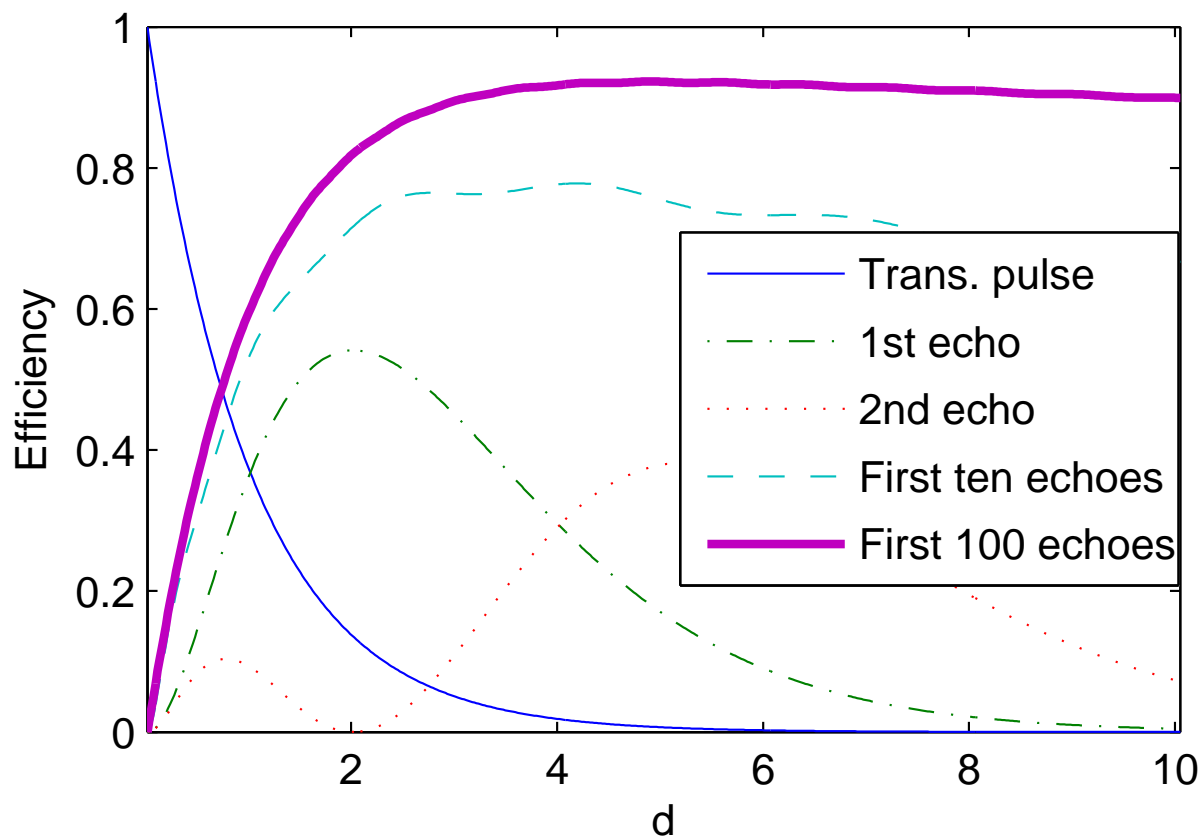


Figure 6: (Color online) Echo efficiency as a function of optical depth for transverse broadening CRIB echo showing the effects of multiple switching. As is shown in the figure efficiencies significantly greater than 54% can be achieved with multiple switching but 100% efficiency is approached relatively slowly as the number of echoes increases. Approximately 100 echoes are needed to achieve greater than 90% efficiency.